to the production of an inactive protein[17,19]. We used a *Dde*I RFLP determined by this point mutation[20] to compare the level of expression of the transgenes with respect to the endogenous gene. Quantification showed that the level of expression per copy of transgene was comparable to that of the endogenous gene (Fig. 3), which indicated copy number dependence and position independence. RT-PCR analysis of additional tissues (data not shown) revealed that the expression of the transgenes had the same tissue-specific pattern as the endogenous gene[15]. The faithful expression of this large and complex transcription unit also argues strongly for integration of unrearranged YAC DNA.

The complete rescue of the albino phenotype of the YRT2 transgenic mice in contrast to mice carrying tyrosinase minigenes[15,17,18], suggests an effect of position and/or the absence of elements necessary for correct expression in the minigene constructs. This could include sequences with properties of dominant control regions, such as those found in the β-globin gene cluster[3] and lysozyme gene[21]. Alternatively, the position-independent and copy number-dependent expression might be due to elements present in the 250 kb construct mediating boundary effects, analogous to those identified in the *Drosophila* genome[22]. One important element might be the DNase I hypersensitive site −15 kb upstream of the tyrosinase gene[23], which is present in B16 mouse melanoma cells but not in mouse NIH3T3 fibroblasts (R. Ganss and G.S., unpublished data). Analysis of deletion derivatives of YRT2 will help to identify the sequences responsible for the correct expression of the tyrosinase gene.

We envisage that YACs covering a locus and sufficient flanking sequences will be of great use for transgenic experiments where correct expression is essential. This will benefit the analysis of large gene clusters in their natural context, such as the globin and the Hox genes, and of far upstream regulatory elements. It will assist the identification of genes by complementation and investigation of long-range regulatory phenomena such as X-inactivation and imprinting. Such analyses will be aided by the ease with which defined mutations and markers can be introduced into YAC constructs by homologous recombination in yeast[24]. □

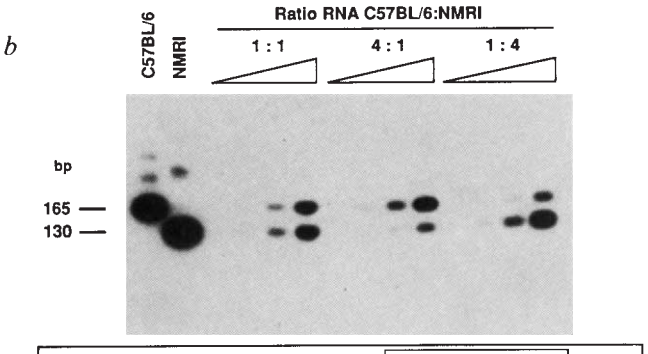

	RNA ratio NMRI: C57BL/6	Expected ratio mutant / wild type	Found ratio mutant / wild type 20	22	24	PCR cycle
Control	1 : 1	1	1.743	1.545	1.181	
	4 : 1	4	3.865	4.433	3.984	
	1 : 4	0.25	0.319	0.281	0.301	

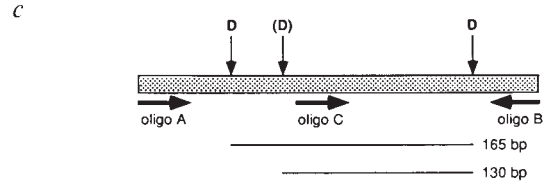

GGATTTGGGGGCCCAAATTGTACAGAGAAGCGAGTCTTGA-3′, bases 398–437 (ref. 31)) was labelled with [γ-^{32}P]ATP and polynucleotide kinase (NEB) for hybridization and detection of the *Dde*I RFLP. Quantification of the bands was made by a Phosphoimager (Molecular Dynamics).

Received 21 January; accepted 19 February 1993.

1. Palmiter, R. D. & Brinster, R. L. *A. Rev. Genet.* **20,** 465–499 (1986).
2. Jaenisch, R. *Science* **240,** 1468–1474 (1988).
3. Grosveld, F., Blom van Assendelft, G., Greaves, D. R. & Kollias, G. *Cell* **51,** 975–985 (1987).
4. Burke, D. T., Carle, F. G. & Olson, M. V. *Science* **236,** 806–812 (1987).
5. Pachnis, V., Pevny, L., Rothstein, R. & Constantini, F. *Proc. natn. Acad. Sci. U.S.A.* **87,** 5109–5113 (1990).
6. Gnirke, A. *et al. EMBO J.* **10,** 1629–1634 (1991).
7. Gnirke, A. & Huxley, C. *Somat. Cell molec. Genet.* **17,** 573–580 (1991).
8. Eliceiri, B. *et al. Proc. natn. Acad. Sci. U.S.A.* **88,** 2179–2183 (1991).
9. Strauss, W. M. & Jaenisch, R. *EMBO J.* **11,** 417–422 (19&2).
10. Schedl, A. *et al. Nucleic Acids Res.* **20,** 3073–3077 (1992).
11. Larin, Z., Monaco, A. P. & Lehrach, H. *Proc. natn. Acad. Sci. U.S.A.* **88,** 4123–4127 (1991).
12. Smith, D. R., Smyth, A. P. & Moir, D. T. *Proc. natn. Acad. Sci. U.S.A.* **87,** 8242–8246 (1990).
13. Ruppert, S., Müller, G., Kwon, B. & Schütz, G. *EMBO J.* **7,** 2715–2722 (1988).
14. Hogan, B., Constantini, F. & Lacy, E. *Manipulating the Mouse Embryo* (Cold Spring Harbor Laboratory Press, New York 1986).
15. Beermann, F. *et al. EMBO J.* **9,** 2819–2826 (1990).
16. Ruppert, S. thesis, Ruprecht Karls Univ., Heidelberg, Germany (1988).
17. Yokoyama, D. *et al. Nucleic Acids Res.* **18,** 7293–7298 (1990).
18. Tanaka, S., Yamamoto, H. Takeuchi, S. & Takeuchi, T. *Development* **108,** 223–227 (1990).
19. Shibahara, S. *et al. Eur. J. Biochem.* **189,** 455–461 (1990).
20. Jackson, I. J. & Bennett, D. C. *Proc. natn. Acad. Sci. U.S.A.* **87,** 7010–7014 (1990).
21. Stief, A., Winter, D. M., Strätling, W. H. & Sippel, A. E. *Nature* **345,** 341–343 (1989).
22. Kellum, R. & Schedl, P. *Cell* **64,** 941–950 (1991).
23. Porter, S., Larue, L. & Mintz, B. *Devl. Genet.* **12,** 393–402 (1991).
24. Reeves, R. H., Pavan, W. J. & Hieter, P. *Genet. Analyt. Techn. Appl.* **5,** 107–113 (1990).
25. Anand, R., Villasante, A. & Tyler-Smith, C. *Nucl. Acids Res.* **17,** 3425–3433 (1989).
26. Lovell-Badge, R. H. *Teratocarcinoma and Embryonic Stem Cells, a Practical Approach* (ed. Robertson, E. J.) (IRL, Oxford, 1987).
27. Kelsey, G. *et al. Genomics* **14,** 275–287 (1992).
28. Robinson, M. O. & Simon, M. I. *Nucleic Acids Res.* **19,** 1557–1562 (1991).
29. Gaudette, M. F. & Crain, W. R. *Nucleic Acids Res.* **19,** 1879–1884 (1991).
30. Weis, J. H., Tan, S. S., Martin, B. K. & Wittwer, C. T. *Trends Genet.* **8,** 263–264 (1992).
31. Mueller, G., Ruppert, S., Schmid, E. & Schütz, G. *EMBO J.* **7,** 2723–2730 (1988).

ACKNOWLEDGEMENTS. We thank E. Thies and W. Fleischer for technical assistance and C. Schneider for secretarial work, Z. Larin and H. Lehrach (ICRF, London) for screening their YAC library and R. Paro (ZMBH, Heidelberg) and D. Duboule (EMBL, Heidelberg) for reading the manuscript. This work was supported by the Deutsche Forschungsgemeinschaft and the Leibniz Program and the Fonds der Chemischen Industrie.

MAP kinase-related FUS3 from *S. cerevisiae* is activated by STE7 *in vitro*

Beverly Errede*, Anton Gartner†‡, Zhaoqing Zhou*, Kim Nasmyth† & Gustav Ammerer†‡§

* Department of Chemistry, University of North Carolina, Chapel Hill, North Carolina 27599, USA
† Institute of Molecular Pathology, A1030 Vienna, Austria
‡ Institut für Allgemeine Biochemie und Ludwig Boltzmann Forschungsstelle, University of Vienna, A1030 Vienna, Austria

PHEROMONE-STIMULATED haploid yeast cells undergo a differentiation process that allows them to mate[1]. Transmission of the intracellular signal involves threonine and tyrosine phosphorylation of the redundant FUS3 and KSS1 kinases, which are members of the MAP kinase family[2–4]. FUS3/KSS1 phosphorylation depends on two additional kinases, STE11 and STE7 (refs 2, 5, 6). Genetic analyses predict an ordered pathway where STE11 acts before STE7 and FUS3/KSS1 (refs 2, 7). Here we report that STE7 is a dual-specificity kinase that modifies FUS3 at the appropriate sites and stimulates its catalytic activity *in vitro*. From these data and previous genetic results, we argue that STE7 is the physiological activator of FUS3. Recent indications that MAP kinase activators are related to STE7 suggest that signal transduction pathways in many, if not all, eukaryotic organisms use homologous kinase cascades[8–10].

§ To whom correspondence should be addressed.

To study FUS3 phosphorylation *in vitro* we isolated it as a Myc epitope-tagged fusion protein from *Escherichia coli* (Fig. 1*a*). We expressed and isolated two inactive mutant derivatives of FUS3 in a similar way. One has a substitution at the conserved catalytic lysine (FUS3M-R42) and the other has two additional changes at the major phosphorylation sites (FUS3M-R42A180F182). The wild-type FUS3M incorporated radioactive phosphate in autophosphorylation assays but the FUS3M-R42 derivative was inactive (Fig. 1*b*). The autophosphorylation product was different from the *in vivo* phosphorylated FUS3, because the former was modified on serine and tyrosine but not on threonine (Fig. 1*c*).

To see if the STE7 kinase could phosphorylate FUS3, we isolated a Myc epitope-tagged version of STE7 (STE7M) from yeast extracts by immune affinity purification. To eliminate FUS3M autophosphorylation, we used the catalytically inactive FUS3M-R42 protein from *E. coli* as the substrate. Phosphorylation of the FUS3M-R42 protein occurred in the reactions with the active STE7M but not the catalytic lysine substitution mutant, STE7M-R220 (Fig. 2*a*, lanes 1, 2, 4 and 5). There was more FUS3M-R42 phosphorylation when STE7M was isolated from pheromone-induced cells (Fig. 2*a*, lanes 1 and 4). This increase must be attributed to a more active STE7 kinase, because the amount of STE7M was the same in extracts from pheromone-induced and uninduced cells (data not shown). As mentioned, STE11 is a second kinase whose function is necessary for FUS3 modification *in vivo*[2]. Under our assay conditions, immune affinity-purified STE11M kinase did not phosphorylate FUS3M-R42 (data not shown). This provides additional evidence that phosphorylation of FUS3M-R42 is specifically catalysed by STE7M.

A second protein was phosphorylated in the STE7M immune complex kinase assays (Fig. 2). This protein was STE7M, because an N-terminally truncated but still biologically active form of the STE7M kinase (STE7M-ΔS) caused a shift in the position of the signal (Fig. 2*a*, lanes 3 and 6). The absence of other phosphoproteins suggests that no coprecipitating kinase intervenes between STE7 and FUS3.

Phosphorylation of FUS3M-R42 in the assays with STE7M occurred on serine, threonine and tyrosine residues (Fig. 2*b*). Most of the modification must be on the threonine 180 and tyrosine 182 sites of *in vivo* phosphorylation because there was much less ^{32}P incorporation with the FUS3M-R42A180F182 derivative (Fig. 2*c*). We propose therefore that STE7 is a dual specificity kinase sufficient for the threonine and tyrosine phosphorylation of FUS3 (ref. 11).

The effect of pheromone induction on FUS3 kinase activity was investigated using an immune complex assay with a Myc epitope-tagged FUS3 (FUS3M). Myelin basic protein (MBP), a standard substrate for vertebrate MAP kinases, was phosphorylated when FUS3M was immune affinity purified from extracts of induced but not uninduced cells (Fig. 3, lanes 1 and 2). Two lines of evidence show that this stimulation of kinase activity is due to pheromone-induced FUS3 phosphorylation. First, the FUS3M-A180F182 mutant, which has substitutions at both *in vivo* sites of modification, did not phosphorylate MBP (Fig. 3, lanes 5 and 6). Second, treatment of FUS3M with phosphatase 2A abolished phosphorylation of the FUS3-specific substrate (data not shown).

FUS3M was also phosphorylated in the immune complexes prepared from pheromone-induced cells. This cannot be due to autophosphorylation because the signal was actually stronger in immune complexes with the inactive FUS3M-R42 protein (Fig. 3, lanes 3 and 4). Therefore, a second kinase was coprecipitated with FUS3M. We think that this kinase is STE7 because a phosphoprotein with the same mobility as STE7 was observed in the reaction with pheromone-induced FUS3M (Fig. 3, lane 2; see below). Additionally, FUS3M-R42 was not phosphorylated when immune complexes were from extracts of pheromone-induced *ste7*Δ mutant cells (data not shown). Note that FUS3M-R42 was phosphorylated to a considerable extent in extracts from uninduced cells (Fig. 3, lane 4), consistent with previously published *in vivo* data suggesting that the basal level of signal activity is actually higher in cells without functional FUS3 (ref. 2).

FUS3 kinase activity can also be stimulated through its *in vitro* modification by STE7M. For these activation assays we used an N-terminal fragment of the FAR1 protein as a FUS3-specific substrate[12]. This polypeptide is a more sensitive and specific substrate than MBP (M. Peter, A.G., G.A. and

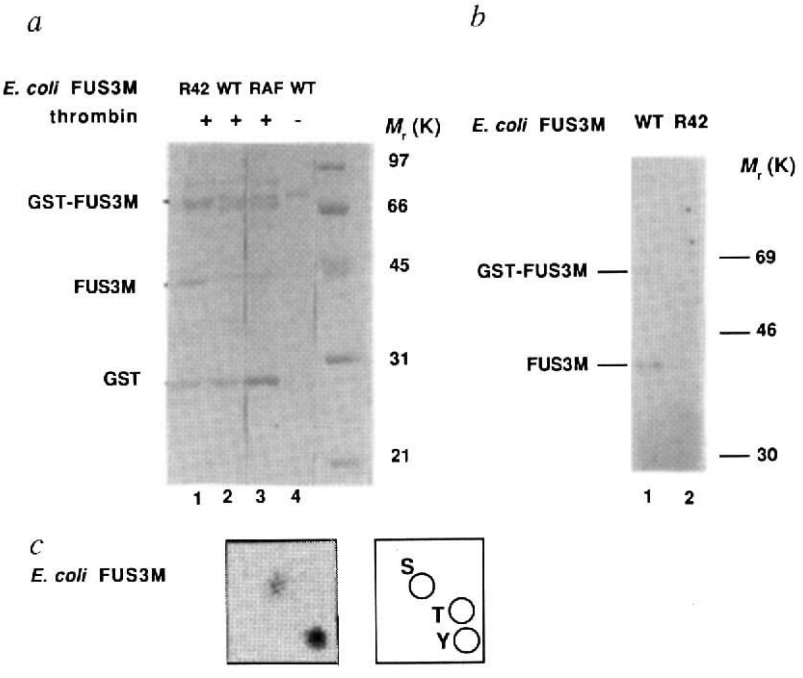

FIG. 1 Purification of FUS3 kinase from *E. coli* and its autocatalytic properties. *a*, Coomassie blue stained gel of SDS–PAGE-fractionated GST fusion proteins purified from *E. coli* after (lanes 1–3) and before (lane 4) cleavage with thrombin. Samples of GST-FUS3M (wt), GST-FUS3M-R42 (R42), and GST-FUS3M-R42A180F182 (RAF) preparations are shown. Position of the GST-FUS3M fusion protein, the cleaved FUS3M protein and the GST polypeptide are indicated. *b*, Autophosphorylation assays with FUS3M (wt) and FUS3M-R42 (R42). *c*, Phosphorimager print of [^{32}P]phospho-amino acids from FUS3M after autophosphorylation (left). Position of phospho-serine (S), -threonine (T) and -tyrosine (Y) standards (right).

METHODS. FUS3M, FUS3M-R42 and FUS3M-R42A180F182 proteins were expressed as GST fusion proteins in a BL21 (DE3) *E. coli* strain using plasmids pGA1965, pGA1944 and pGA1945, respectively. To construct these expression plasmids, the *Nde*I-*Bam*HI fragments encoding tagged FUS3 (FUS3M) and derivatives were isolated from pGA1903, pGA1905 and pGA1932 (ref. 20) and cloned into plasmid pGEX-2T6 (provided by G. Draetta). Except for the addition of an *Nde*I site, pGEX-2T6 is the same as pGEX-2T (ref. 14). Fusion protein synthesis was induced at room temperature and the proteins were purified as described[14]. Autophosphorylation assays were done in a final reaction volume of 20 μl that included 250 ng of purified FUS3M or FUS3M-R42 and 10 μCi [$\gamma^{32}P$]ATP. Kinase assay buffer was as described[15] but β-glycerol phosphate was omitted. After 30 min incubation at 30 °C, reactions were stopped by addition of SDS–PAGE sample buffer[16] and boiling for 3 min. Phosphoproteins were fractionated by SDS–PAGE[16] and visualized by autoradiography of the dried gel. The analysis of FUS3M phospho-amino acids was as previously described[2].

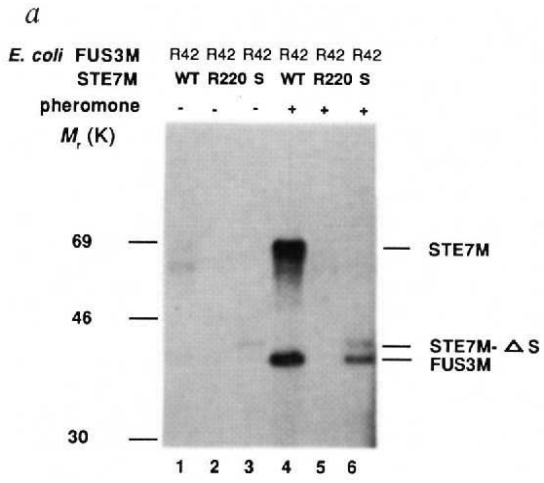

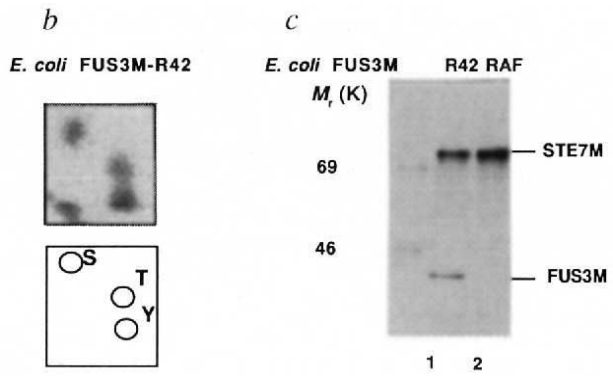

FIG. 2 STE7 phosphorylates FUS3. *a*, Comprison of STE7 kinase activity from uninduced (−) and induced (+) cultures. Immune affinity-purified STE7M (wt), STE7M-R220 (R220) or STE7M-ΔS (S) was present as indicated. Each assay mixture contained 250 ng purified FUS3M-R42 (R42) as substrate. Note that STE7M from pheromone-induced cells is hyperphosphorylated causing it to have a lower mobility than when isolated from uninduced cells (lanes 1 and 4). *b*, Phosphorimager print of [^{32}P]phospho-amino acids in FUS3M-R42 from *a*, lane 4 (top). Migration of phospho-serine (S), -threonine (T) and -tyrosine (Y) standards (bottom). *c*, Comparison of FUS3M-R42 (R42, 250 ng) and FUS3M-R42A180F182 (RAF, 250 ng) as substrates for immune affinity-purified STE7M (wt) from pheromone-induced cells.

METHODS. The plasmids pNC267 and pNC267-R220 for expression of STE7M and STE7M-R220 will be described elsewhere[20]. The *STE7M-ΔS* allele was constructed by site-directed mutagenesis using the *STE7* phagemid pNC318 as source of template DNA and oligonucleotide 5′-CGTATCTTTCAGATCTGCG-CCTTCTATTCG as the mutagenic primer[17]. The resulting plasmid (pNC346) has a deletion in *STE7* that encompasses codons 45–170. The plasmid pNC348 was constructed by transferring the *STE7M-ΔS* allele from pNC346 as a *Sal*I–*Hin*dIII fragment to YEplac112 (ref. 18). Yeast strain K2149, which was used for expression of STE7M or STE7M-R220, has been described[2]. Yeast strain E929-6C-35 (*STE7Δ FUS3 KSS1 bar1Δ*), which was used for expression of STE7M-ΔS, is isogenic to strain E929-6C (ref. 5). Where pheromone induction is indicated, cultures were exposed to 50 nM α-factor for 1.5 h. Extracts were prepared as described[15] but with modified stop and lysis buffer (50 mM Tris, pH 7.5, 150 mM NaCl, 5 mM EDTA, 1% Nonidet P-40 (NP-40), 50 mM NaF, 30 mM $Na_2H_2P_2O_7$, 15 mM 4-nitrophenylphosphate, 0.1 mM ortho-vanadate, 1 mM PMSF, 40 μg ml^{-1} aprotinin and 20 μg ml^{-1} leupeptin). For immune affinity purification of STE7M or derivatives, 100 μg of the specified extract was incubated with 4 μg of Myc1-9E10 antibodies for 1 h on ice[19]. The antibody–antigen complexes were incubated with protein A sepharose beads (10 μl packed volume) at 4 °C for 1.5 h. The adsorbed immune complexes were washed five times in buffer A (50 mM Tris pH7.5, 150 mM NaCl, 5 mM EDTA, 1% NP-40, 15 mM 4-nitrophenylphosphate, 0.1 mM ortho-vanadate), three times in buffer B (25 mM MOPS pH 7.2, 15 mM 4-nitrophenylphosphate, 0.1 mM ortho-vanadate) and once in buffer B plus 15 mM $MgCl_2$. Substrate phosphorylation assays with the immune complexes and analysis of phosphorylation products were as described in Fig. 1, except that 2 μCi of [γ-^{32}P]ATP was used per reaction.

I. Herskowitz, manuscript in preparation). Addition of purified FUS3M and FAR1 proteins to STE7M immune complexes from extracts of pheromone-induced *kss1 fus3* double mutant cells resulted in FAR1 phosphorylation (Fig. 4*a*, lane 3). No modification of FAR1 occurred without the addition of FUS3M (Fig. 4*a*, lanes 1 and 2). When FUS3M was present with the inactive STE7M-R220, we observed much less FAR1 phosphorylation (Fig. 4*a*, lane 4). We suppose that the autophosphorylated form of FUS3 could be responsible for this minor activity.

STE7 is also a substrate of the FUS3 kinase. STE7M was phosphorylated in reactions where the wild-type FUS3M has been activated (Fig. 4*b*, lane 3) but not in reactions with the inactive FUS3M-R42 (Fig. 4*b*, lanes 1 and 2). This is consistent with the observation that hyperphosphorylation of STE7 *in vivo* depends on an active FUS3 or KSS1 kinase[7]. The role of this reciprocal phosphorylation of STE7 by FUS3 is unclear but it could be part of an attenuation mechanism. This proposal is consistent with a higher signal activity in *fus3 kss1* double mutant cells compared with wild-type cells as indicated by the relative amounts of FUS3-R42 phosphorylation (ref. 2 and Fig. 3, lane 4). Additionally, STE7M kinase catalysed more FUS3-R42 phosphorylation when it was isolated from a *fus3 kss1* strain compared with a wild-type strain (Fig. 4*c*). Because the same amount of STE7 was present in the two extracts (data not shown), STE7 seems to be more active when isolated from cells without FUS3 or KSS1.

It has been noted that peptide sequences obtained from purified *Xenopus* and rabbit skeletal muscle MAP kinase activators show similarities to the STE7 sequence[8–10]. The case for a close relationship between MAP kinase kinase and STE7 has been made even stronger by recent results[21]. This suggests that the kinase cascade we have characterized in yeast will be

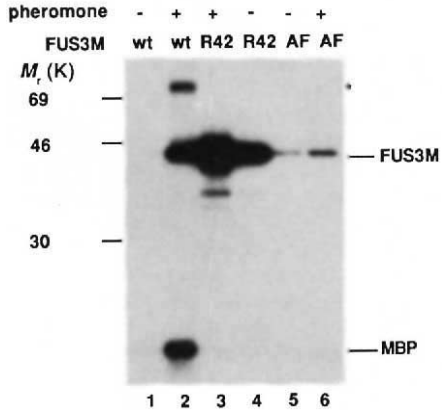

FIG. 3 Pheromone potentiates FUS3 kinase activity. Results of phosphorylation assays with 10 μg of bovine myelin basic protein (MBP) added to immune affinity-purified FUS3M (wt), FUS3M-R42 (R42) and FUS3-T180Y182 (AF) from uninduced (−) or pheromone-induced (+) cultures. The positions of FUS3M and MBP are indicated. The asterisk marks one coimmune-precipitated protein that is only phosphorylated in reactions with pheromone-induced and catalytically active FUS3M.

METHODS. FUS3M (pGA1903), FUS3M-R42 (pGA1905) and FUS3M-A180F182 (pGA1906) were expressed in yeast strain K2314 (*STE7 fus3Δ kss1Δ bar1Δ*)[2]. Where pheromone induction is indicated, cultures were exposed to 50 nM α-factor for 1 h. Extract preparation, immune affinity purification of FUS3M (or derivatives) and phosphorylation assays were essentially as described in Fig. 2.

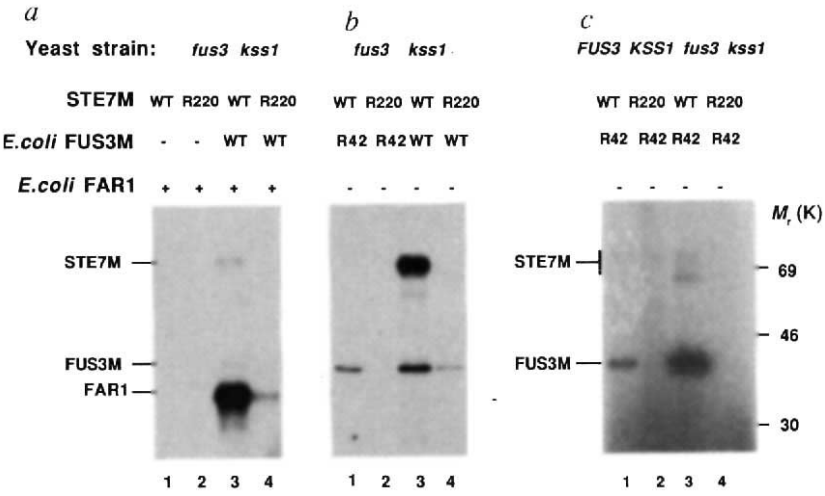

FIG. 4 STE7 reconstitutes activation of the FUS3 kinase. *a*, Phosphorylation assays showing STE7 stimulates FUS3-dependent phosphorylation of FAR1, STE7M (wt, pNC318) or STE7M-R220 (R220, pNC318-R220) was immune affinity purified from pheromone-treated cultures of K2314 (*fus3 kss1*). FUS3M (250 ng) produced and purified from *E. coli* was either present (wt) or absent (−) from the reactions. The target substrate, an N-terminal fragment of FAR1 (250 ng) was present (+) in all assays. The positions of phosphorylated FAR1 fragment, FUS3M and STE7M and STE7M are indicated. *b*, Phosphorylation assays showing that activated FUS3 phosphorylates STE7. Purified FUS3M (wt; 250 ng) or FUS3M-R42 (R42; 250 ng) was added to STE7M (wt) and STE7M-R220 (R220) isolated as specified in *a*. *c*, Comparison of STE7M kinase activity after isolation from *FUS3 KSS1* or *fus3 kss1* genetic backgrounds. Phosphorylation assays with 250 ng of purified FUS3M-R42 as substrate and immune affinity-purified STE7M (wt) or STE7M-R220 (R220) from pheromone-induced cultures of strain K2180 (lanes 1 and 2) and strain K2314 (lanes 3 and 4).

METHODS. The plasmids pNC318 and pNC318-R220 for expression of STE7M and STE7M-R220, respectively, will be described elsewhere[20]. Yeast strains K2314 (*STE7 fus3Δ kss1Δ bar1Δ*) and K2180 (*STE7 FUS3 KSS1 far1Δ bar1Δ*) are isogenic with strain K2149 (ref. 2). Expression and purification of the N-terminal FAR1 fragment (encompassing amino acids 1–268) used as substrate will be described elsewhere (M. Peter *et al.*, manuscript in preparation). Phosphorylation assays were as described in Fig. 2.

found in many if not all eukaryotic cells. In yeast, the cascade consists of the STE11, STE7 and FUS3/KSS1 kinases whose equivalents in mammals may be the Raf kinase (or perhaps another kinase equivalent to STE11), a STE7-like MAP kinase activator and MAP kinase[8–10,13]. □

Received 17 September 1992; accepted 18 January 1993.

1. Marsh, L., Neiman, A. M. & Herskowitz, I. A. *A. Rev. Cell Biol.* **7,** 699–728 (1991).
2. Gartner, A., Nasmyth, K. & Ammerer, G. *Genes Dev.* **6,** 1280–1292 (1992).
3. Elion, M. E., Brill, J. A. & Fink, G. R. *Proc. natn. Acad. Sci. U.S.A.* **88,** 9392–9396 (1991).
4. Boulton, T. G. *et al. Science* **249,** 476–489 (1990).
5. Rhodes, N. L., Conell, L. & Errede, B. *Genes Dev.* **4,** 1862–1874 (1990).
6. Teague, M. A., Chaleff, D. T. & Errede, B. *Proc. natn. Acad. Sci. U.S.A.* **83,** 7371–7375 (1986).
7. Stevenson, B. J., Rhodes, N., Errede, B. & Sprague, G. F. Jr *Genes Dev.* **6,** 1293–1304 (1992).
8. Kosado, H. *et al. EMBO J.* **11,** 2903–2908 (1992).
9. Nakielny, S., Campbell, D. G. & Cohen, P. *FEBS Lett.* **308,** 183–189 (1992).
10. Wu, J. *et al. Biochem. J.* **285,** 701–705 (1992).
11. Lindberg, R. A., Quinn, A. M. & Hunter, T. *Trends biochem. Sci.* **17,** 114–119 (1992).
12. Chang, F. & Herskowitz, I. *Cell* **63,** 999–1011 (1990).
13. Howe, L. R. *et al. Cell* **71,** 355–342 (1992).
14. Smith, D. B. & Johnson, K. S. *Gene* **61,** 31–40 (1988).
15. Surana, U. *et al Cell* **65,** 145–161 (1991).
16. Laemmli, U. K. *Nature* **227,** 680–685 (1970).
17. Kunkel, T. A. *Proc. natn. Acad. Sci. U.S.A.* **82,** 488–492 (1985).
18. Geitz, R. D. & Sugino, A. *Gene* **74,** 527–534 (1988).
19. Evan, G. I., Lewis, G. K., Ramsay, G. & Bishop, J. M. *Molec. cell. Biol.* **5,** 3610–3616 (1985).
20. Zhou, Z., Gartner, A., Cade, R., Ammerer, G. & Errede, B. *Molec. cell. Biol.* (in the press).
21. Crews, C. M., Alessandrini, A. & Erickson, R. L. *Science* **258,** 478–480 (1992).

ACKNOWLEDGEMENTS. We thank H. Tkadletz for help in preparing the figures, G. Schaffner and co-workers for oligonucleotide synthesis and DNA sequencing, L. Ballou for sound advice concerning STE7 isolation and assay conditions and L. Ballou, K. Bloom, L. Dirik, B. Stevenson and B. Yashar for comments on the manuscript. A.G. and G.A. were supported by a grant from the Austrian Fonds zur Förderung der wissenschaftlichen Forschung. B.E. and Z.Z. were supported by grants from the United States Public Health Service.

Pituitary hormone FSH directs the CREM functional switch during spermatogenesis

Nicholas S. Foulkes, Florence Schlotter, Paul Pévet* & Paolo Sassone-Corsi†

Laboratoire de Génétique Moléculaire des Eucaryotes du CNRS, U184 de l'INSERM, Faculté de Médecine, 11 rue Humann, 67085 Strasbourg, France
* Neurobiologie des Fonctions Rythmiques et Saisonnieres, CNRS URA 1332, 12 rue de l'Université, 67000 Strasbourg, France

THE CREM (cyclic AMP-responsive element modulator) gene encodes multiple regulators of the cAMP-transcriptional response by alternative splicing[1]. A developmental switch in CREM expression occurs during spermatogenesis, whereby CREM function is converted from an antagonist to an activator (CREMτ; ref. 2) which accumulates to extremely high levels from the premeiotic spermatocyte stage onwards. To define the physiological mechanisms controlling the CREM developmental switch, we have hypophysectomized rats and observed the extinction of CREMτ expression in testis, thereby demonstrating a central role of the pituitary–hypothalamic axis. We then used the seasonal-dependent modulation of spermatogenesis in hamsters to dissect the hormonal programme controlling this developmental process. By this approach, combined with direct administration of pituitary-derived hormones, we have established that follicle-stimulating hormone (FSH) is responsible for the CREM switch. FSH appears to regulate CREM expression by alternative polyadenylation, which results in a dramatic enhancement of transcript stability.

We have shown that the amount of the CREM transcript increases dramatically from the pachythene spermatocyte stage onwards and encodes the activator CREMτ instead of the antagonists[2]. In mouse the switch occurs between days 13 and 14 (Fig. 1*a*, lanes 1–5). This functional switch is conserved in other species at an equivalent stage during spermatogenesis (hamster and rat, see lanes 6–9). As testicular functions are under the control of the pituitary–hypothalamic axis[3,4], we tested whether surgical removal of the pituitary gland could affect CREM expression. CREMτ expression is dramatically reduced in the adult rat one week after surgery (Fig. 1*b*, lanes 2, 7, 8). Removal of other endocrine glands has no detectable effect (lanes 1 and 3). To test whether there is a pituitary control of the developmental switch of CREM in testis, we hypophysectomized prepubertal rats. No equivalent switch in CREM expression or transcript accumulation was detected during subsequent development (Fig. 1*b*, lanes 9–11 and 12, 13). Thus a functional pituitary is necessary for the switch and maintenance of CREM transcript abundance and spicing. In addition, we analysed *Hox-1.4* expression, which is also developmentally regulated during spermatogenesis[5]. *Hox-1.4* induction is almost coincidental with that of CREMτ (Fig. 1*a*). *Hox-1.4* expression was

† To whom correspondence should be addressed.